Features in the ion emission of Cu, Al, and C plasmas produced by ultrafast laser ablation

T. J. Kelly, T. Butler, N. Walsh, P. Hayden, and J. T. Costello

---

Articles you may be interested in

Emission features of femtosecond laser ablated carbon plasma in ambient helium
J. Appl. Phys. **113**, 163305 (2013); 10.1063/1.4803096

Dynamics of the plumes produced by ultrafast laser ablation of metals
J. Appl. Phys. **108**, 043309 (2010); 10.1063/1.3475149

Ablation and plasma emission produced by dual femtosecond laser pulses
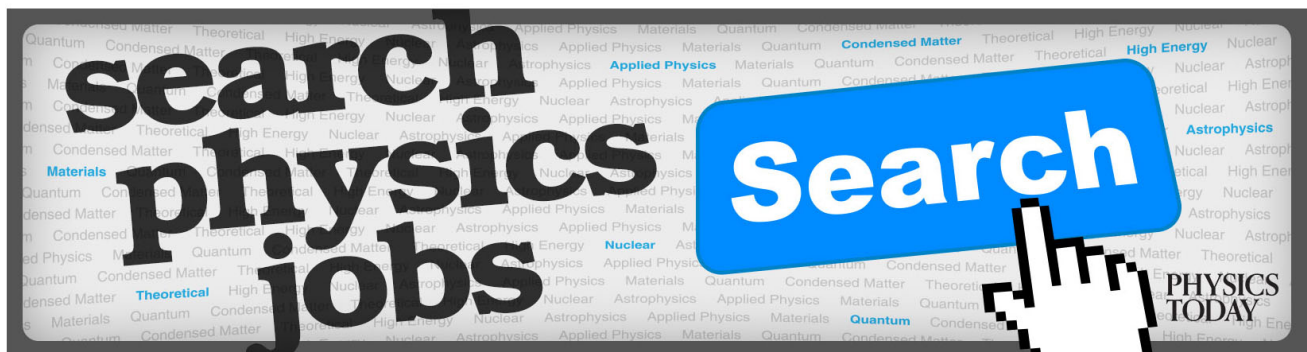J. Appl. Phys. **104**, 113520 (2008); 10.1063/1.3040082

Particle emission from tantalum plasma produced by 532 nm laser pulse ablation
J. Appl. Phys. **100**, 093306 (2006); 10.1063/1.2358400

Ion Emission from Laser-Produced Plasmas
Phys. Fluids **10**, 2091 (1967); 10.1063/1.1762418

Features in the ion emission of Cu, Al, and C plasmas produced by ultrafast laser ablation

T. J. Kelly,[1,a)] T. Butler,[2] N. Walsh,[1] P. Hayden,[1] and J. T. Costello[1]
[1]*National Centre for Plasma Science and Technology, School of physical sciences, Dublin City University, Glasnevin, Dublin 9, Ireland*
[2]*Centre for Advanced Photonics and Process Analysis (CAPPA), Cork Institute of Technology, Cork, Ireland*

The bi-modal nature of charge integrated ion kinetic energy distributions, which result from ultrafast laser produced plasmas, is discussed in this paper. A negatively biased Faraday cup was used as a charge collector to measure ion distributions from three different solid targets that had been irradiated with an ultrafast laser in the fluence range 0.1–1 J/cm^2. A bi-modal time of flight distribution is found for all three targets (C, Al, and Cu). In the case of the metallic targets (Al and Cu), high- and low-kinetic energy peaks exhibit quite different dependencies on laser fluence, whereas for the semi-metallic target (C), both peaks scale similarly with ultrafast laser fluence. The results are discussed within the framework of a one dimensional capacitor model resulting in ion acceleration. © 2015 AIP Publishing LLC. [http://dx.doi.org/10.1063/1.4937800]

I. INTRODUCTION

The removal of mass from a solid target using a laser, known as laser ablation, is a technique that is almost as old as the laser itself. The invention of the pulsed, high powered laser heralded the arrival of the field of laser produced plasmas (LPPs) as it is today.[1] In early experiments, LPPs were formed with lasers whose pulse duration was typically microseconds or nanoseconds in duration. The advent of chirped pulse amplification[2] allowed for the generation of moderately intense laser pulses whose duration was on the order of tens of femtoseconds. This was a revolutionary step in the formation of LPPs. Regardless of the choice of laser, or target, the first interaction between the laser and the target is with the electrons. The laser imparts energy to the electrons through some absorption process (for nanosecond lasers, this tends to be inverse bremsstrahlung, and for femtosecond lasers, this tends to be multiphoton ionization). The electrons then transfer this energy to the target lattice. The time it takes for this to occur is typically tens of picoseconds for most metals.[3] This is one reason that the invention of lasers with ultrashort pulse durations was a revolutionary step in the formation of LPPs. In the long pulse laser case, the laser field is still present as the electrons transfer energy to the target lattice. In the ultrashort laser case, the laser field terminates long before the energy transfer occurs. Knowledge of the ion energy distribution of laser produced plasmas is important should the plasma be used in various industrial and academic applications such as pulsed laser deposition,[4] laser induced breakdown spectroscopy,[5] laser assisted mass spectrometry,[6] ion implantation,[7] and light source generation.[8] Given the fall in cost of ultrafast lasers, along with the fact that they couple more efficiently to the target, further growth in the use of ultrafast laser ablation based applications can be expected, and so an increasingly deeper understanding of all apposite aspects will be required including the ion energy.

The formation of plasmas with non-Maxwellian distributions is indicative of non-thermal components within the plasma. Early experiments and theoretical efforts ascribed the deviation from Maxwellian behaviour to the formation of a space charge within the plasma. LPPs formed with a long pulse laser have been observed with non-Maxwellian distributions since the 1970s.[9] Various mechanisms have been proposed to explain this observation including the formation of double layers through, possibly, hot electrons generated by three body recombination.[10] The non-Maxwellian distribution sometimes manifested itself as a double peaked structure in the ion time of flight signal. Other experiments noticed that a double peaked structure was predominantly observed in high Z targets for the long pulse laser case. Thus, the double peaked structure was attributed to acceleration of highly charged components.[11]

By contrast, in the case of ultrafast laser ablation, the formation of a non-thermal component seems intrinsic to the whole process because the electrons in the skin layer are heated and ionized before any thermalization can occur. Indeed, a double peaked structure in the time of flight signal was observed in initial experiments in ultrafast laser ablation.[12] A comparison of ultrafast and nanosecond laser ablation at similar fluences to the work presented in this article showed that in aluminium, the plume produced by nanosecond ablation showed a Maxwellian distribution, while the plume formed by ultrafast laser ablation contained a non-Maxwellian component and a Maxwellian component.[13] The fluence dependence of these two components was studied, and it was found that the Maxwellian component has a sub-linear dependence on fluence, while the non-Maxwellian component has a super-linear dependence. The Maxwellian component was also found to be of a lower kinetic energy than the non-Maxwellian component. Thus, the Maxwellian component is attributed to thermal ionization, whereas the

a)Electronic mail: thomas.kelly9@mail.dcu.ie

22, 123112-1

non-Maxwellian component is attributed to space charge effects within the plume.[12,14] The exact nature of the formation of the non-Maxwellian peak is somewhat under debate. For example, some theoretical and experimental studies suggest electrostatic removal of ions as a possible explanation for the non-Maxwellian peak.[13] In other studies, it is suggested that perhaps the rising edge of the laser pulse creates a nascent vapour, which is then heated by the back edge of the laser pulse creating a fast electron component.[12] These electrons then accelerate a fraction of ions in the plume. Other studies attribute the fast peak to light contaminants on the target surface.[15] A recent, comprehensive study used a multi-diagnostic technique to unambiguously clarify the existence of a fast ion component from the bulk plasma, and the results were explained in relation to ambi-polar diffusion, similar to the interpretation in this article.[16,17]

In this article, we report on the results of an experiment where the time of flight signals resulting from ultrafast laser ablation of three different solid targets were measured. The results are then interpreted as being due to acceleration of a small component of the thermal plume. Scaling laws are derived to explain how the kinetic energy and relative ion yield change with fluence and target choice. The article is arranged as follows: In Section II, the experiment is described; in Section III, the case of copper ablation is studied in detail and a theoretical model is described to help explain the data. This is then used to explain the observations from ablation of aluminium and carbon targets.

II. EXPERIMENTAL

The experimental system used in this work is shown in Figure 1.

A Ti:Sapphire laser system was used to create a laser produced plasma from three different targets: copper, aluminium, and carbon. It comprised a Kerr lens mode-locked Ti:Sapphire oscillator (Coherent Micra 5) used to seed a regenerative amplifier (Coherent Legend Elite). The laser was operated at its fundamental wavelength of 800 nm, which was monitored periodically throughout the experiment by means of an optical spectrometer. The laser pulse width at the output of the laser was measured by means of a second order autocorrelator to be 34 fs, and this was also monitored periodically throughout the experiment. The total additional pulse broadening through various optical elements was measured to be 36 fs giving a final pulse width of 70 fs. This is still far below the ion electron coupling time for the targets used. Ions from the three targets were collected by means of a home built Faraday cup that was placed 4 cm from the target. The collector of the Faraday cup was a further 2 cm from the entrance aperture to give an effective distance of 6 cm. Plasma ions were measured at laser fluences ranging from 0.1 to 1 J/cm^2, which was controlled with a pulse-width preserving laser attenuator. The spot size was estimated to be 6×10^{-4} cm$^2 \pm 0.2 \times 10^{-4}$ cm^2 by measuring the burn pattern on a fresh silicon surface following multiple laser shots as a function of fluence and determining the spot size (ω_o) on a semi-log plot.[18] The peak and average fluences are then given by $F_{peak} = E/\omega_o$ and $F_{avg} = 0.5F_{peak}$, respectively (for an assumed Gaussian beam shape), where E is the laser pulse energy. The ion signal was read out through a Koopman circuit[19] and was stored on a fast oscilloscope. A shot to shot analysis revealed that the initial few shots (10 or so) on the target resulted in a time of flight signal that contained multiple peaks and varied hugely from shot to shot. After 10 or so shots on the same spot, a bi-modal structure appeared, which was stable for 100s of laser shots. This was the same for all targets. Thus, all experiments reported here are for an average of 16 laser shots after the target had been cleaned with 10 laser shots. A trigger-wait function allowed for 10 shots to be fired on the target before the oscilloscope started recording. The oscilloscope was triggered by means of a photodiode in the beamline. A typical ion trace measured by the experiment is shown in Figure 2. The experiment was housed in a vacuum chamber and evacuated to a pressure of 1×10^{-5} mbar by means of a turbomolecular pump.
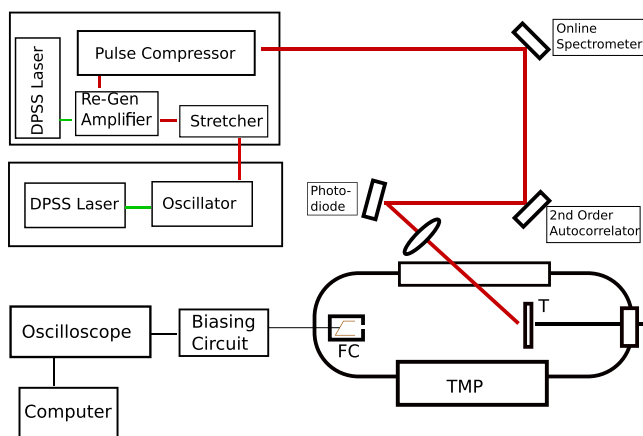

FIG. 1. Schematic of the experimental setup. The target (T) is housed in a vacuum chamber, which is evacuated by a turbo molecular pump (TMP). The Faraday cup (FC) is placed 6 cm away, and the signal is read out using a biasing circuit, displayed on an oscilloscope, and finally stored on a computer. Laser light leakage from the final routing mirror is used to trigger a photodiode to give the experimental time zero. The spectrum and autocorrelation of the pulse are measured periodically through leakage from other routing mirrors.
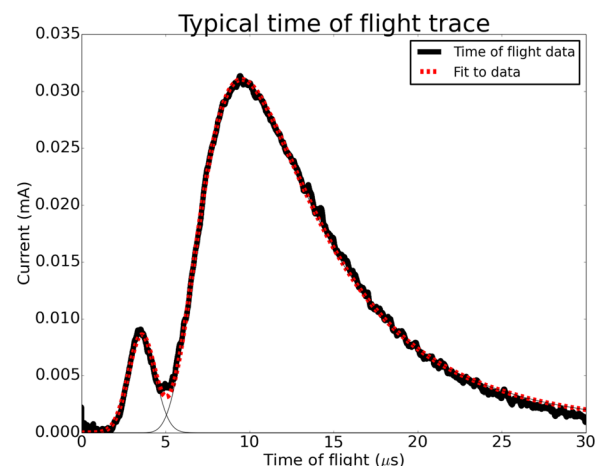

FIG. 2. Typical ion trace obtained during the experiment. The bold black data are the experimental data and the red are a fit to the data using Eq. (1). This is a time of flight trace for a copper plasma at a fluence of 1 J/cm^2.

The bi-modal structure has been seen in many laser experiments before and has been attributed to different mechanisms. For instance, the high kinetic energy peak has been attributed to accelerated ions,[12] low mass impurities,[15] and supra-thermal ion emission.[13] In our experiment, we observe that the bi-modal structure appears in all targets after the surface has been cleaned with ten laser shots. The high kinetic energy peak survives for 100 s of laser shots and, in fact, after a few hundred laser shots, the signal begins to die away. The decay of the fast peak was found to be in relative proportion to the decay of the slow peak. The signal was parameterized using the copper target as this gave the clearest bi-modal structure.

III. RESULTS AND DISCUSSION

A. Characterization of ion signal

The ion emission from a copper target was used to parametrize the data in a way that could be used to develop a physical model of the experiment. Figure 3 shows the Faraday cup signal from a copper target at different laser fluences.

From the data, there are two distinct features in the ion signal. First, a fast ion peak that grows with increasing laser fluence is present followed by a broader, slower peak that also grows in intensity with increasing laser fluence. The fast peak was best characterized by fitting it to a Gaussian distribution of the form $f(t) = Ae^{-\left(\frac{t-t_0}{\sqrt{2}\sigma}\right)^2}$. The slow peak was best described by a shifted Maxwell-Boltzmann (SMB) distribution. This indicates that the fast peak is non thermal in nature, while the slow peak is a thermal component. This observation is in line with previous ultrafast laser ablation experiments.

The total signal was fit to a model function of the form

$$I(t) = A_1 t^{-n} \exp\left[-\beta\left(\frac{L}{t} - v_d\right)^2\right] + A_2 e^{-\left(\frac{t-t_0}{\sqrt{2}\sigma}\right)^2}. \quad (1)$$

The value of n is typically either $n = 3$ or $n = 4$ with the case of $n = 3$ referring to a SMB distribution,[20] which
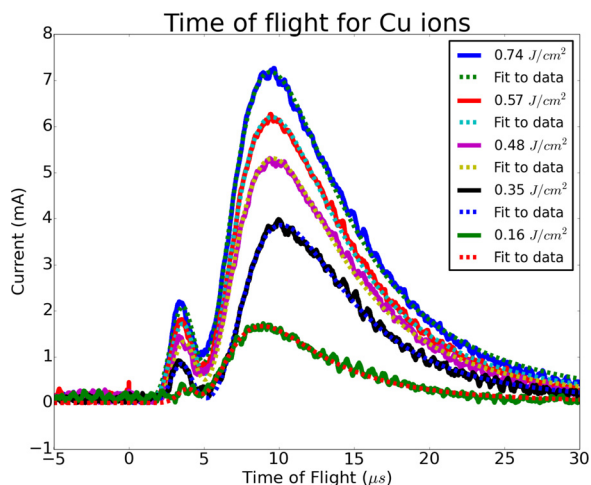

FIG. 3. Ion time of flight distributions for copper plasma with varying laser fluence values.

describes a one dimensionally expanding laser plasma plume. The case of $n = 4$ usually describes a high density plasma, which includes the formation of a Kundsen Layer.[21] In this experiment, it was found that the best fit occurred with $n = 3$. This indicates that the plasma plume is of low density and can be described as a one dimensional expansion. Previous studies on the angular distributions of ions from plasmas produced by ultrafast laser ablation have shown a very narrow angular spread compared to the dimensions of the experiment.[15,22] Thus, the assumption of 1-D expansion is probably valid.

The value of L was set equal to the target-cup distance and kept fixed in the fitting routine. The fitted parameter, t_0, was used to determine the arrival time of the fast peak and was thus used in calculating the kinetic energy of the fast peak. This parameter's behaviour with fluence and target is discussed in Figure 9. The β parameter in Eq. (1) is used to determine the ion temperature as $\beta = m_i/2kT_i$. It was found that the temperature T_i was in the range 0.5–2 eV for all targets and increased very gently with laser fluence. Both σ and v_d were found to have weak dependences on laser fluence. v_d increased with the mass of target chosen. The integrated current derived from the fits to each plasma component is used to give the relative contribution to the total signal from both the fast and slow components. Figure 4 shows how the yield of each component changes with laser fluence.

The slow component shows a sub-linear dependence on fluence, whereas the fast component shows a super-linear dependence. This indicates that the slow component is produced by thermal means. Previous reports have shown that the solution to the two temperature model predicts that the thermal component of a plasma plume produced by ultrafast laser ablation should have two separate sub-linear dependencies on fluence depending on whether or not the laser fluence exceeds the ablation threshold: defined as the fluence at which the laser heats the electrons in the skin layer to a temperature exactly equal to the Fermi energy. The super-linear dependence of the fast peak has been reported before, many times.[12] As mentioned in the Introduction, there are a number of possibilities as to the nature of the fast peak. First, the possibility of low-Z contaminants is ruled out as previously discussed in the experimental section. Similarly, the possibility of the rising edge of the laser pulse creating a nascent vapour and ionizing this to give an accelerated component is discounted as only a small fraction of the 70fs laser pulse would be available to interact with any nascent vapour. Thus, it is concluded that the most likely explanation for the appearance of the fast peak is acceleration due to a space charge effect in the plasma.

B. Aluminium and carbon

Measurements were also made on an aluminium target under the same conditions as the copper target. The time of flight results are shown in Figure 5.

The data show a small shoulder on the high kinetic energy side of the time of flight signal. Any attempt to fit the data to a Maxwellian only distribution resulted in a poor fit or unphysical fitting parameters. To accurately model the
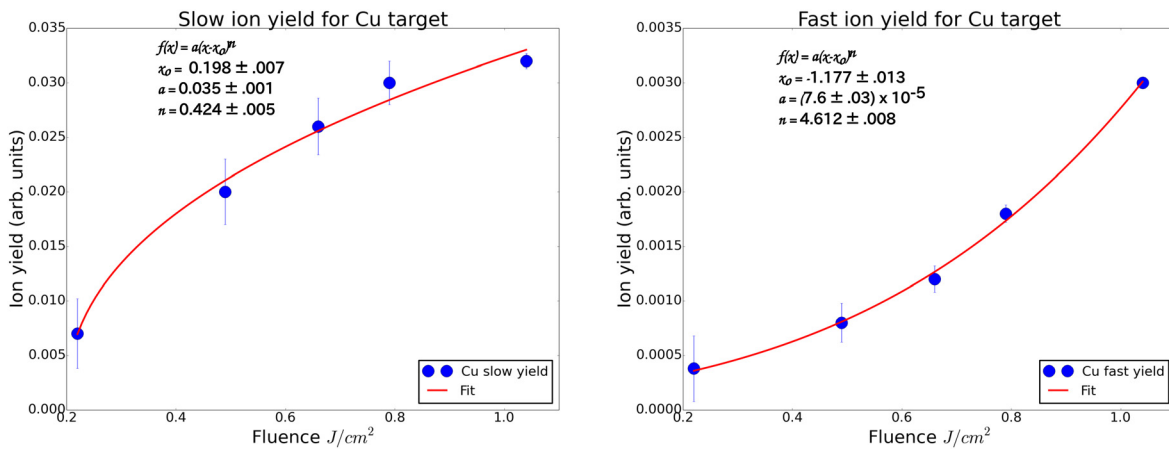
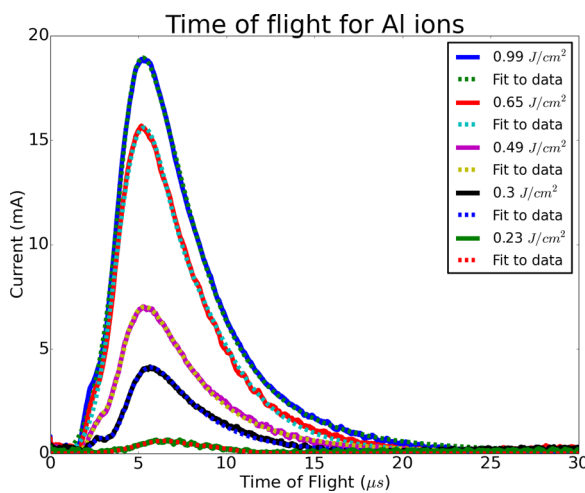FIG. 4. Slow and fast peak behaviour with changing laser fluence.

FIG. 5. Ion time of flight distributions of aluminium plasma for various fluences.

data, a high kinetic energy non-Maxwellian component was needed. Thus, the data were fit to the same distribution as in Eq. (1). The fast and slow peak yield is plotted in Figure 6.

Much like the copper data, the low kinetic energy peak appears to have a sub-linear dependence with fluence indicating a thermal plasma component. On the other hand, the

fast peak behaves linearly with fluence. The time of flight signal for carbon, measured under the same conditions, is shown in Figure 7.

In Figure 7, there is no obvious "second peak" as it were. However, any attempt to fit the data to a Maxwellian distribution only resulted in non physical fitting parameters in all cases except for the lowest fluence. When a high kinetic energy, non Maxwellian component was included in the fit, like the copper and aluminium data, the data were fitted well. The fluence dependence of the yield of fast and slow components, which resulted from the fit, is shown in Figure 8.

IV. DISCUSSION

Before discussing the results in detail, it might be helpful to draw together some observations from Section III.

1. All targets show evidence of a non-Maxwellian (fast peak) component in the ion velocity distribution and a Maxwellian (slow peak) component.
2. The temporal separation of the two peaks grows with atomic mass.
3. The yield ratio of fast peak ions to slow peak ions is very small in Al and Cu (0.2), whereas for C the ratio is quite high (0.7).
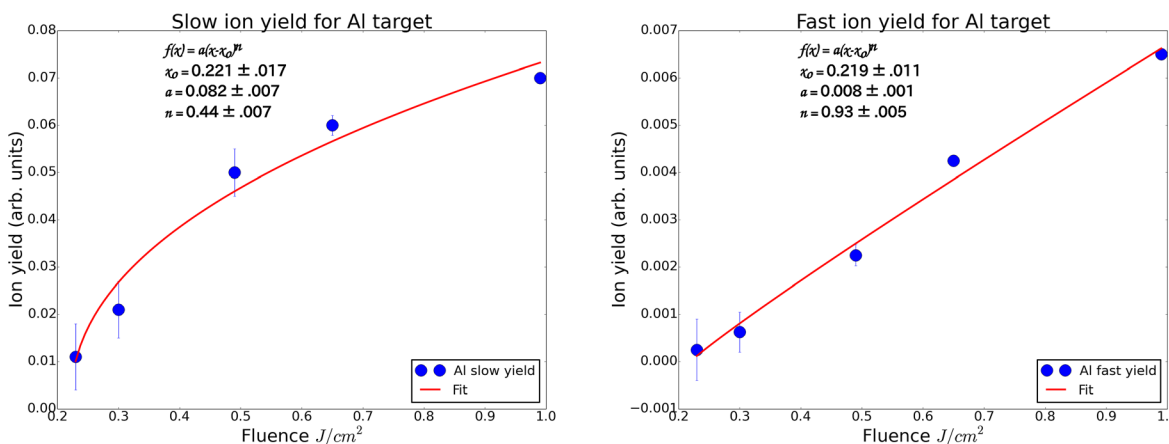

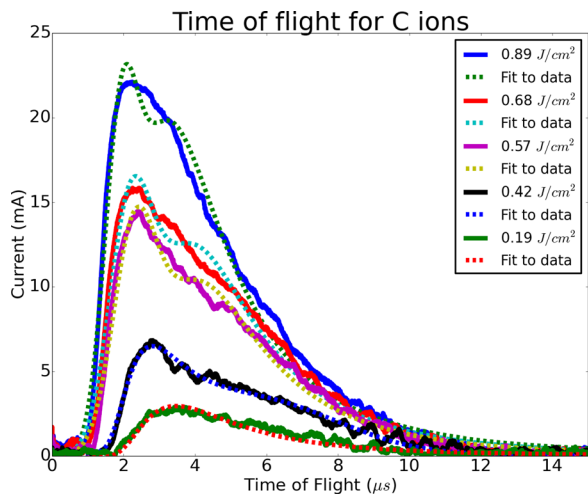FIG. 6. Slow and fast peak behaviour with changing laser fluence for an aluminium target.

FIG. 7. Ion time of flight distributions of carbon plasma for various fluences.

4. The kinetic energy of the fast peak grows with laser fluence as does the temperature of the Maxwellian component. The kinetic energy of the fast peak also varies with target choice, whereas the temperature of the Maxwellian component is ≈1–2 eV for all targets over the fluence range studied. Figure 9 shows the kinetic energy of the fast peak for all targets.
5. For all targets, the slow peak grows sub-linearly with laser fluence. The fast peak fluence dependence transitions from super-linear to sub-linear as the atomic mass decreases.

The data are modeled as follows.[23,24] The laser penetrates into the target to some depth given by

$$\delta = \frac{c}{\omega k}, \tag{2}$$

where ω is the laser frequency, c is the speed of light, and k is the extinction co-efficient of the material under consideration. The electrons within a volume equal to the product of the laser spot size and the penetration depth absorb energy from the laser through multiphoton ionization. The electrons gain energy in excess of the Fermi energy and escape from the target. Their escape kinetic energy is found as follows. A

one dimensional heat equation describes the electron heating process

$$C_e(T_e)n_e \frac{\partial T_e}{\partial t} = -\frac{\partial Q}{\partial x}, \tag{3}$$

where C_e is the electron specific heat capacity, n_e is the electron number density, T_e is the electron temperature (expressed in energy), and Q is the laser source term with $Q = AI_o e^{-2x/\delta}$, where A is the absorption co-efficient, I_o is the laser intensity, and δ is the penetration depth. At low temperatures, the electron specific heat is given by $C_e = \pi^2 T_e/2\epsilon_F$.[23] For high temperatures, the specific heat approaches that of an ideal gas and has a constant value $C_e = \frac{3}{2}$. We treat the electrons as being in conditions close to an ideal gas because they are heated almost instantaneously, and the density does not change during the laser pulse. Thus, the solution for the electron temperature is found by integrating Eq. (3) over time

$$T_e = \frac{4}{3}\frac{AI_o t}{\delta n_e}e^{-2x/\delta}. \tag{4}$$

For most metals (such as copper and aluminium), the absorption coefficient is much less than one and the ratio A/δ is constant. Thus, the electron temperature in the skin layer is inversely proportional to the number density of electrons. It can thus be inferred that a lower number density of electrons will result in a higher electron temperature in the skin layer. This is qualitatively similar to saying that a lower number density of electrons results in a lower Fermi energy for a metallic solid. The electrons will then escape from the target with a kinetic energy given by Eq. (5)

$$KE_e = T_e - \phi. \tag{5}$$

Substituting in values for the aluminium and copper targets gives fast electrons with kinetic energies of 34 eV (copper) and 13 eV (aluminium). This gives escape velocities of 7.8×10^5 m/s and 3×10^5 m/s, respectively. A mechanism that can explain the data is the development of a time dependent electric field arising from the separation of the fast electrons and a positively charged thermal ion component. In this
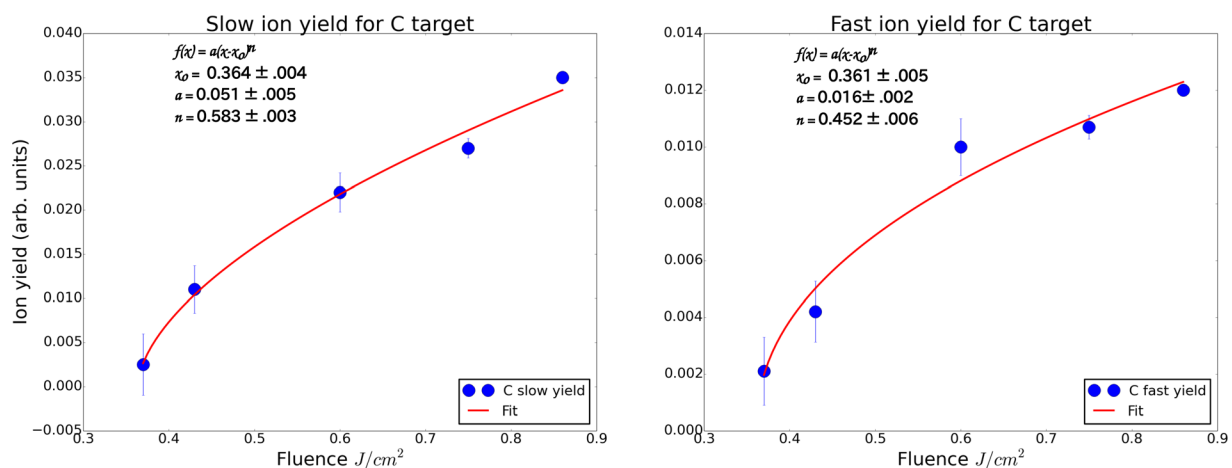

FIG. 8. Slow and fast peak behaviour with changing laser fluence for a carbon target.
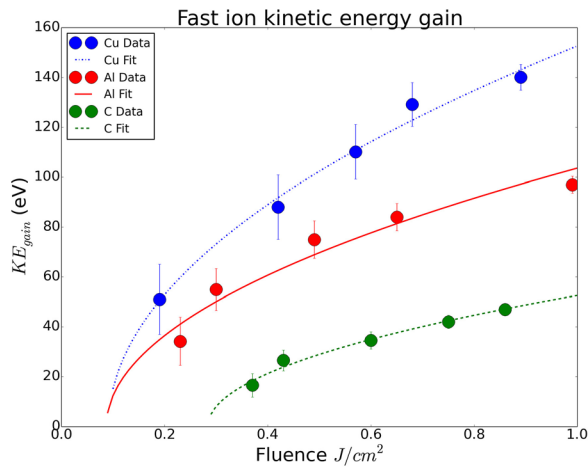
FIG. 9. Kinetic energy of fast component with fluence for all targets. The data points for each target were fitted with a function $f(x) = a(x - x_o)^{0.5}$, where x is the laser fluence.

scenario, the laser penetrates into the target, heating electrons to a temperature described by Eq. (4). The heated electrons in the skin layer mean that the lattice is out of thermal equilibrium. After the laser pulse, the electrons begin transferring energy to the lattice such that the electron and ion temperatures equalize. If the energy of the electrons is greater than the Fermi energy, they will escape from the target, and if the energy of the ions is greater than the binding energy, a thermal plume will be created. The drift speed of the electrons will be much higher than the ions due to their respective inertia, and so a space charge separation occurs. This space charge effect causes a time dependent ambipolar electric field to develop between the electrons and the ions. This field will perform work on both the ions and electrons with the effect of speeding the ions up and slowing the electrons down until their speeds are equal. The overall effect of this is that the ions gain kinetic energy, and it is this process that is the most likely explanation for the fast ion peak present in Figures 3, 5, and 7. At this point, the plasma plume consists of two parts: A low kinetic energy, quasi-neutral thermal component, and a high kinetic energy structure that contains fast electrons and accelerated ions. This model explains qualitatively the trends seen in aluminium and copper. The kinetic energy gained by the ions can be estimated by treating the fast electron and accelerated ion component as two plates of a capacitor as has previously been used to good effect.[12,16] The size of the plates, S, is estimated as the laser spot size, and the charge density of each capacitor plate can be written as $\sigma_o = qN_e/S$, where N_e is the number of charged particles on the plate (i.e., number of fast electrons or number of accelerated ions assuming a singly ionized target). The electric field between these two "plates" is given by $E = \sigma_o/\epsilon = qN_e/\epsilon S$, where ϵ is the dielectric constant. The gain in kinetic energy of the ions is found by the work-energy theorem to be

$$\frac{1}{2}mv^2 = KE_{gain} = qV = qE\lambda_d, \tag{6}$$

which gives

$$KE_{gain} = q^2 N_e \lambda_d / \epsilon S. \tag{7}$$

It can be seen from Eq. (7) that the gain in kinetic energy will be proportional to the Debye length, λ_d, which is the spatial separation between the accelerated ions and fast electrons. The value of N_e is estimated experimentally from the total integrated ion signal and found to be $\sim 6 \times 10^{10}$ for both aluminium and copper. The debye length is found from $\lambda_d = \sqrt{KE_e/m_e\omega_{pe}^2}$. As seen before, the electron kinetic energy KE_e is inversely proportional to the electron density and proportional to the electron temperature (which itself is proportional to the laser intensity), and so it can be assumed that $\lambda_d \propto n_e^{-1}$ and $\lambda_d \propto I^{1/2}$, where I is the laser intensity. Thus, it can be concluded that the kinetic energy gained by the ions should grow with laser intensity and be inversely proportional to the kinetic energy of the escaping electrons. Thus, it is expected that the copper ions will gain more energy than aluminium, which is supported in Figure 9.

The discussion has thus far deliberately only focused on aluminium and copper. The fast peak in carbon is found to be consistently and significantly lower in energy than aluminium and copper. This is explained by the fact that while aluminum and copper are metals, carbon is a semi-metal and as such has negligible density of states at the Fermi level. Thus, in order to remove electrons from carbon, extra energy must be added to first promote the electrons to the conduction band. This energy is roughly equivalent to the ionization potential of carbon. Thus, the carbon data are qualitatively explained by saying that the fast electrons have much less kinetic energy when they escape from the target because extra energy is required to create free carriers. Finally, the relative yield is much higher for carbon than for aluminium and copper. This is explained by the fact that the skin depth is much larger for carbon due to the much smaller extinction ratio at the laser wavelength. Thus, the laser penetrates more deeply into the target, and so more electrons participate in the acceleration process.

The fast ion yields are shown to be super-linear for aluminium and copper yet sub-linear for carbon. One possible explanation for this is that the fast electron yield should have a super-linear dependence on fluence as the dominant heat absorption process in the skin layer is multi-photon ionization. Thus, if one ion is accelerated for every one electron, the ion signal should be non-linear too. However, if the ions are accelerated from a thermal component, which has a sub-linear dependence on fluence, then the fast ion yield should grow in fluence with some exponent, which is some blend of both the sub and super-linear processes. Intuitively, one would expect that the greater the kinetic energy gained by the ions, the more the super-linear process should dominate the exponent. This perhaps qualitatively explains the correlation between fast electron kinetic energy and the value of the exponent in the fluence behaviour of the targets, which is seen in the experiment.

V. CONCLUSIONS

Ion measurements were made on three solid targets ablated with an ultrafast laser using a Faraday cup. The three targets were aluminium, copper, and carbon. In all three cases, a bi-modal ion kinetic energy structure was observed.

It is proposed that this arises due to ion acceleration from a space charge layer within the plasma. Qualitative relative dependencies of the fast ion kinetic energy and yield ratio are found to be in agreement with the observed data.

ACKNOWLEDGMENTS

[1]L. Radziemski and D. Cremers, *Laser-Induced Plasmas and Applications* (CRC Press, New York and Basel, 1989).

[2]D. Strickland and G. Mourou, Opt. Commun. **56**, 219 (1985).

[3]P. Corkum, F. Brunel, N. Sherman, and T. Srinivasan-Rao, Phys. Rev. Lett. **61**, 2886 (1988).

[4]T. Donnelly, S. Krishnamurthy, K. Carney, N. McEvoy, and J. Lunney, Appl. Surf. Sci. **254**, 1303 (2007).

[5]M. Oba, Y. Maruyama, K. Akaoka, M. Miyabe, and I. Wakaida, Appl. Phys. A **101**, 545 (2010).

[6]B. Fernandez, F. Claverie, C. Pecheyran, and O. Donard, TrAC Trends Anal. Chem. **26**, 951 (2007).

[7]E. Wornya, J. Wolowski, B. Kralikova, J. Krasa, L. Laska, M. Pfeifer, K. Rohlena, J. Skala, V. Perina, F. Broody, R. Hopfl, and H. Hora, Rev. Sci. Instrum. **71**, 949 (2000).

[8]P. Yeates and E. Kennedy, J. Appl. Phys. **108**, 093306 (2010).

[9]S. Eliezer and H. Hora, Phys. Rep. **172**, 339 (1989).

[10]N. Bulgakova, A. Bulgakova, and O. Bobrenok, Phys. Rev. E **62**, 5624 (2000).

[11]A. O'Connor, O. Morris, and E. Sokell, J. Appl. Phys. **109**, 073301 (2010).

[12]S. Amoruso, X. Wang, C. Altucci, C. de Lisio, M. Armenante, R. Bruzzese, N. Spinelli, and R. Velotta, Appl. Surf. Sci. **186**, 358 (2002).

[13]B. Verhoff, S. Harilal, and A. Hassanein, J. Appl. Phys. **111**, 123304 (2012).

[14]S. Amoruso, X. Wang, C. Altucci, C. de Lisio, M. Armenante, R. Buzzese, and R. Velotta, Appl. Phys. Lett. **77**, 3728 (2000).

[15]T. Donnelly, J. Lunney, S. Amoruso, R. Bruzzese, X. Wang, and X. Ni, J. Appl. Phys. **108**, 043309 (2010).

[16]K. Anoop, X. Ni, X. Wang, S. Amoruso, and R. Bruzzese, Laser Phys. **24**, 105902 (2014).

[17]K. Anoop, M. Pole, R. Bruzzese, S. Amoruso, and S. Harilal, J. Appl. Phys. **117**, 083108 (2015).

[18]J. M. Liu, Opt. Lett. **7**, 196 (1982).

[19]T. Kelly, Eur. J. Phys. **36**, 055041 (2015).

[20]S. Singh, C. Fallon, P. Hayden, M. Mujawar, P. Yeates, and J. Costello, Phys. Plasmas **21**, 093113 (2014).

[21]D. Doria, A. Lorusso, F. Belloni, and V. Nassisi, Rev. Sci. Instrum. **75**, 387 (2004).

[22]J. Freeman, S. Harilal, P. Diwakar, B. Verhoff, and A. Hassanein, Spectrochim. Acta, Part B **87**, 43 (2013).

[23]E. Gamaly, A. Rode, B. Luther-Davies, and V. Tikhonchuk, Phys. Plasmas **9**, 949 (2002).

[24]E. Gamaly, A. V. Rode, V. T. Tikhonchuck, and B. Luther-Davies, Appl. Surf. Sci. **197–198**, 699 (2002).